ECOLOGY

10.1126/sciadv.1501392

Spatial models reveal the microclimatic buffering capacity of old-growth forests

Sarah J. K. Frey,[1]* Adam S. Hadley,[1] Sherri L. Johnson,[2] Mark Schulze,[1] Julia A. Jones,[3] Matthew G. Betts[1]*

Climate change is predicted to cause widespread declines in biodiversity, but these predictions are derived from coarse-resolution climate models applied at global scales. Such models lack the capacity to incorporate microclimate variability, which is critical to biodiversity microrefugia. In forested montane regions, microclimate is thought to be influenced by combined effects of elevation, microtopography, and vegetation, but their relative effects at fine spatial scales are poorly known. We used boosted regression trees to model the spatial distribution of fine-scale, under-canopy air temperatures in mountainous terrain. Spatial models predicted observed independent test data well (r = 0.87). As expected, elevation strongly predicted temperatures, but vegetation and microtopography also exerted critical effects. Old-growth vegetation characteristics, measured using LiDAR (light detection and ranging), appeared to have an insulating effect; maximum spring monthly temperatures decreased by 2.5°C across the observed gradient in old-growth structure. These cooling effects across a gradient in forest structure are of similar magnitude to 50-year forecasts of the Intergovernmental Panel on Climate Change and therefore have the potential to mitigate climate warming at local scales. Management strategies to conserve old-growth characteristics and to curb current rates of primary forest loss could maintain microrefugia, enhancing biodiversity persistence in mountainous systems under climate warming.

INTRODUCTION

Macroscale climate patterns are well known to influence range-wide suitability for biota. However, local-scale climate (hereafter microclimate) is often most relevant to animal behavior and demography (*1*). Reconciling this mismatch between global climate models and the scale at which organisms experience their environment should therefore improve our understanding of biodiversity responses to climate change (*2*, *3*). Furthermore, in heterogeneous mountain landscapes with complex thermal regimes (*4*), climate-sensitive species have the potential to disperse to, and persist in, favorable microclimatic conditions (*5*). Coarse-scale climate data are not as accurate for predicting trends in mountains, influencing our ability to assess climate impacts (*6*). Identification of factors that generate particular microclimates will help focus conservation efforts to lessen the impacts of climate change on biodiversity (*7*), which are expected to be particularly substantial in mountainous regions (*8*). However, to date, the coarse resolution of most land cover and climate data has precluded such analysis (*9*).

The decoupling of the surface temperature conditions from those of the troposphere is commonly attributed to two main factors in mountainous areas: (i) local air-flow dynamics, such as cold air drainage and pooling, and (ii) variations in slope and aspect (microtopography) (*7*). However, vegetation also has the potential to influence microclimatic patterns via its effects on solar radiation, wind exposure, interception of precipitation, and retention of understory humidity. Indeed, the influence of vegetation on microclimate has long been recognized (*10*, *11*) and is the reason why long-term weather stations are situated in open areas. Unfortunately, such sampling strategies have precluded inferences about the relative influences of microtopography and vegetation structure on mediating microclimate (*2*).

If particular vegetation structural characteristics can abate the effects of regional climate change (*12*), land management has the potential to either amplify or buffer these effects on biodiversity (*13*). Given the rapid global changes in land use (*14*), it is critical to understand the degree to which management influences microclimate. An increasing proportion of the world's forests are secondary, transformed forests (*14*, *15*). Therefore, it is essential to understand the implications of secondary forests for climate and biodiversity. Here, we examine whether the structural characteristics present in old-growth forests (for example, heterogeneous canopies, high biomass, and complex vertical structure) increase site-scale thermal buffering capacity over more structurally simple, but mature plantation forest stands. The substantial biomass associated with western old-growth forests might be expected to result in slower rates of warming during summer months (*16*). Alternatively, the closed and homogeneous canopy conditions of old (>50-year-old) forest plantations could prevent rapid site-level warming through reduced solar radiation, thereby moderating climate (*17*). Although previous work has examined the effects of substantial differences in canopy cover on microclimate (*4*, *18*–*22*), to our knowledge, ours is the first broad-scale test of whether subtle changes in forest structure due to differing management practices influence forest temperature regimes (Fig. 1). Given that old-growth forests continue to decline globally (*23*) and that plantations continue to proliferate (*24*), understanding microclimatic impacts is of great conservation importance.

In 2012 and 2013, we collected understory air temperatures at high spatial resolution across a complex mountainous landscape at the H. J. Andrews Experimental Forest (HJA) in Oregon, USA. We obtained fine-resolution (5 m) data on topography and vegetation structure using LiDAR (light detection and ranging). We then used machine-learning techniques [that is, boosted regression trees (BRTs)] to map predicted

[1]Forest Biodiversity Research Network, Department of Forest Ecosystems and Society, Oregon State University, Corvallis, OR 97331, USA. [2]U.S. Forest Service, Pacific Northwest Research Station, Corvallis, OR 97331, USA. [3]Geography, College of Earth, Ocean, and Atmospheric Sciences (CEOAS), Oregon State University, Corvallis, OR 97331, USA.
*Corresponding author. E-mail: sarah.frey@oregonstate.edu, sjkfrey@gmail.com (S.J.K.F.); matt.betts@oregonstate.edu (M.G.B.)

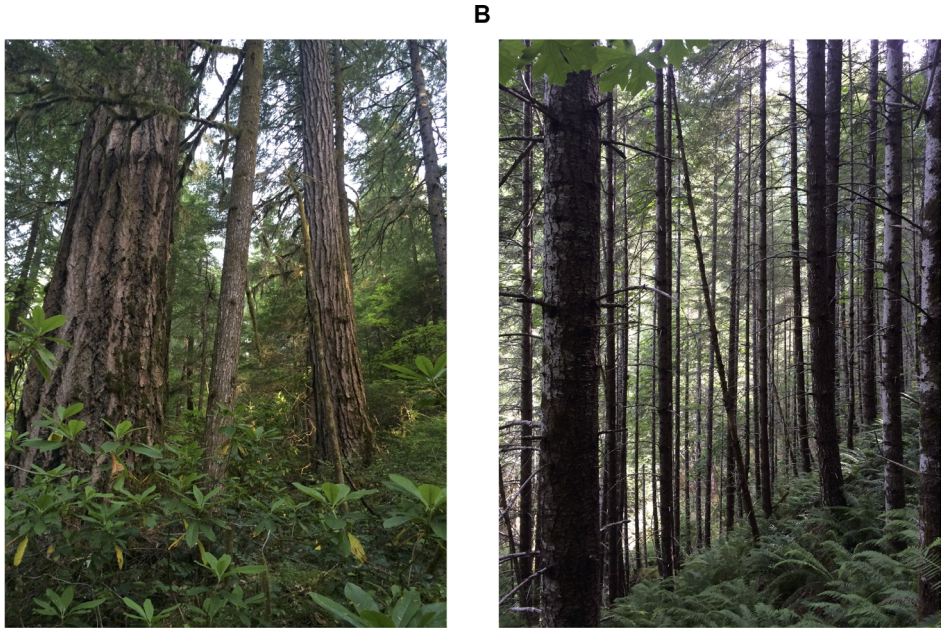

Fig. 1. The high biomass, tall canopies, and vertical structure of old-growth forests are associated with lower spring maximum temperatures than in mature plantations. Photos of old-growth (**A**) and mature plantation (**B**) forest stands at the H. J. Andrews Experimental Forest (HJA) in Oregon, USA. [photo credit: Matthew Betts, Oregon State University].

thermal properties at the landscape scale and to test the hypothesis that vegetation structure mediates under-canopy microclimates.

RESULTS

All models performed well when tested on independent data (table S1). The cross-validation correlations were high, showing substantial congruence between training and test data [mean ± SD (range): 2012, r = 0.87 ± 0.09 (0.69 to 0.98); 2013, r = 0.84 ± 0.11 (0.64 to 0.96)]. This performance was not caused by spatial dependency in the data (table S1). These results indicate that BRTs, which are now used extensively in species distribution models (SDMs) (*25*), seem to offer a powerful new approach to examining spatial distributions in abiotic conditions. As in SDM applications, the advantage of such machine-learning methods lies in their capacity to incorporate many independent variables and their flexibility to include nonlinearities and variable interactions. Although parametric alternatives are available (for example, generalized linear models), our results indicate that BRTs also represent a promising option for distinguishing the relative importance (RI) of complex climate drivers and for generating detailed spatial climate predictions (fig. S1).

Elevation was the dominant predictor for most of the temperature metrics (Fig. 2), including cumulative degree days (CDDs); monthly minimum, maximum, and mean temperatures during spring-summer (April to June); and minimum temperature of the coldest month (Fig. 3A). High-elevation sites were generally cooler and had fewer CDDs. Microtopographic features showed high RI for predicting CDDs during winter-spring (January to March; RI 2012: 45.9%; RI 2013: 53.9%) and maximum temperature of the warmest month (RI 2012: 37.9%; RI 2013: 32.2%; Fig. 3C). Steeper, exposed, south-facing sites were generally warmer and more variable, and accumulated more CDDs (fig. S2).

Among all temperature metrics, maximum temperature of the warmest month (RI 2012: 35.5%; RI 2013: 39.8%) and variability in weekly spring-summer temperature (RI 2012: 36.7%; RI 2013: 10.2%) were most strongly influenced by vegetation structure (that is, canopy height, biomass, understory cover, and vertical structure; Fig. 2). Vegetation structure also had a strong effect on mean monthly maximum temperature from April to June (RI 2012: 20.4%; RI 2013: 18.9%; Fig. 2). Furthermore, vegetation structure was an important predictor for temperature variability (RI 2012: 28.9%; RI 2013: 31.6%) and CDDs during winter (RI 2012: 31.2%; RI 2013: 34.3%). Sites with old-growth forest traits (for example, taller canopies, higher biomass, and more complex vertical structure) had reduced temperatures and greater temperature stability (fig. S2). Old-forest characteristics, such as taller canopies, more canopy cover >10 m, and biomass >500 Mg/ha, reduced maximum temperature of the warmest month and mean monthly maximum temperature from April to June (fig. S3, A to C). Old-forest traits also had an important influence on climate variability; for example, increased coefficient of variation in canopy height and greater midcanopy cover (2 to 10 m) both reduced variability in mean weekly temperature from January to March (fig. S3, D and E). Areas with the lowest biomass variability (for example, even-aged stands such as plantations) showed more microclimate variability in this winter-spring transition (fig. S3F).

However, topographic position (valleys versus topographically exposed sites) appeared to accentuate the effect of forest structure; exposed sites with low variability in biomass (for example, plantation stands) accumulated the most degree days (fig. S4A). A vegetation-elevation interaction revealed that maximum monthly temperature during spring-summer was lowest at high elevations with high amounts of canopy cover surrounding a site (fig. S4C). In both years and for most temperature metrics, variables at the local scale (25-m radius) had a greater relative influence than variables averaged across a 250-m radius [overall average RI at the local scale (25 m) across all metrics: 2012: 60.7 ± 10%;

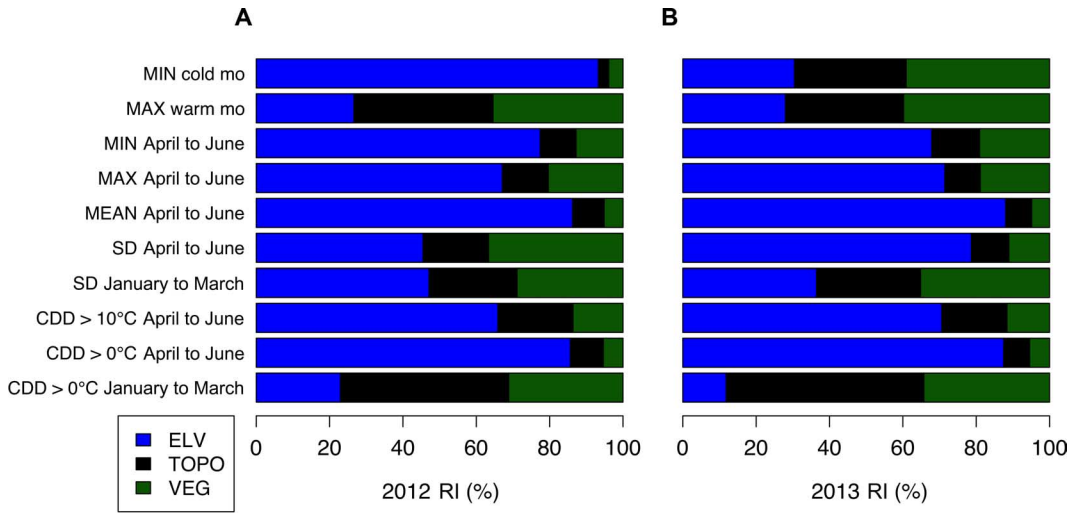

Fig. 2. Relative influence (RI) of variables describing elevation (ELV), microtopography (TOPO), and vegetation structure (VEG) for each temperature metric. RI values for 2012 (**A**) and 2013 (**B**) were derived from the number of times each variable was selected in the process of model building using boosted regression trees (BRTs). Overall, elevation had the strongest influence on air temperature patterns in the HJA, but microtopography and vegetation also exerted important effects, particularly for maximum temperature of the warmest month, variability measures, and cumulative degree days (CDD) in the winter-spring transition.

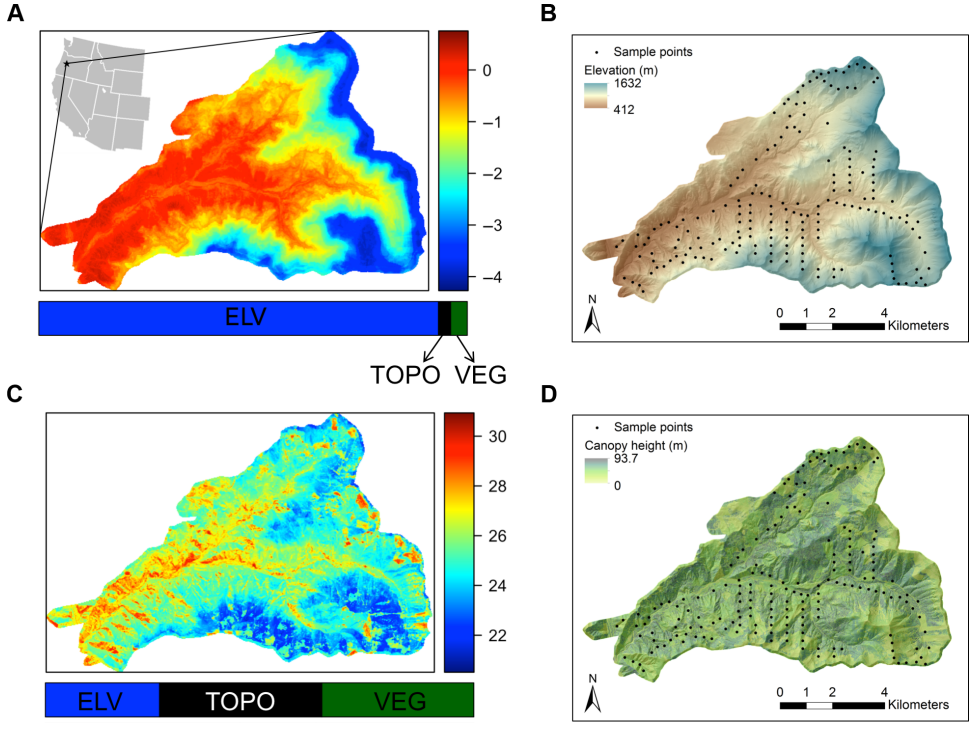

Fig. 3. Spatially predicted maps of minimum temperature of the coldest month and maximum temperature of the warmest month (in degrees Celsius) based on BRT models. Minimum temperatures (**A**) were primarily influenced by elevation (**B**), but maximum temperatures (**C**) were primarily a function of vegetation and microtopography (**D**). Maps of the elevational gradient (B; in meters) and canopy height (D; in meters) based on LiDAR from 2008 at the HJA. Black dots show the 183 temperature sampling locations. The location of the HJA in the western United States is shown in (A).

2013: 60.4 ± 10.1%]. However, vegetation metrics tended to have more influence at the broader (250-m) spatial scale (fig. S5). Despite interannual differences in the RI of variables, we found remarkable between-year consistency in both predicted and observed under-canopy thermal conditions across sites (7 of 10 variables with $r > 0.9$; table S2 and figs. S6 and S7). This interannual consistency in site-level conditions, which occurred despite substantial differences in annual climatic conditions, lends support to the notion that thermally buffered sites may provide temporally consistent refugia for biodiversity (*7*).

Despite being well suited to prediction given our complexity of input variables, BRTs do not provide information on effect sizes (that is, regression coefficients) (*25*). Therefore, we used principal components analysis (PCA) to integrate vegetation structure variables into a reduced number of components (table S3). The first two principal components of the PCA explained 74.7% of the variability [principal component 1 (PC1) = 44.7%; principal component 2 (PC2) = 30%]. The first component (PC1) strongly reflected a gradient in forest structure from closed-canopy plantations to mature/old-growth forests (Figs. 1 and 4A); this gradient represents the predominant forest types on federal land in the region (*26*). Sites with low PC1 values had less biomass (mean and SD), lower canopies (mean and SD), and less cover (2 to 10 and >10 m) (table S3). The individual LiDAR metrics effectively distinguished between plantation sites and mature/old-growth forest sites (table S4); a discriminant function analysis (*27*) showed that prediction accuracy was 85.3% for plantation sites and 90.4% for mature/old-growth forest sites. Furthermore, our LiDAR metrics were congruent with previously

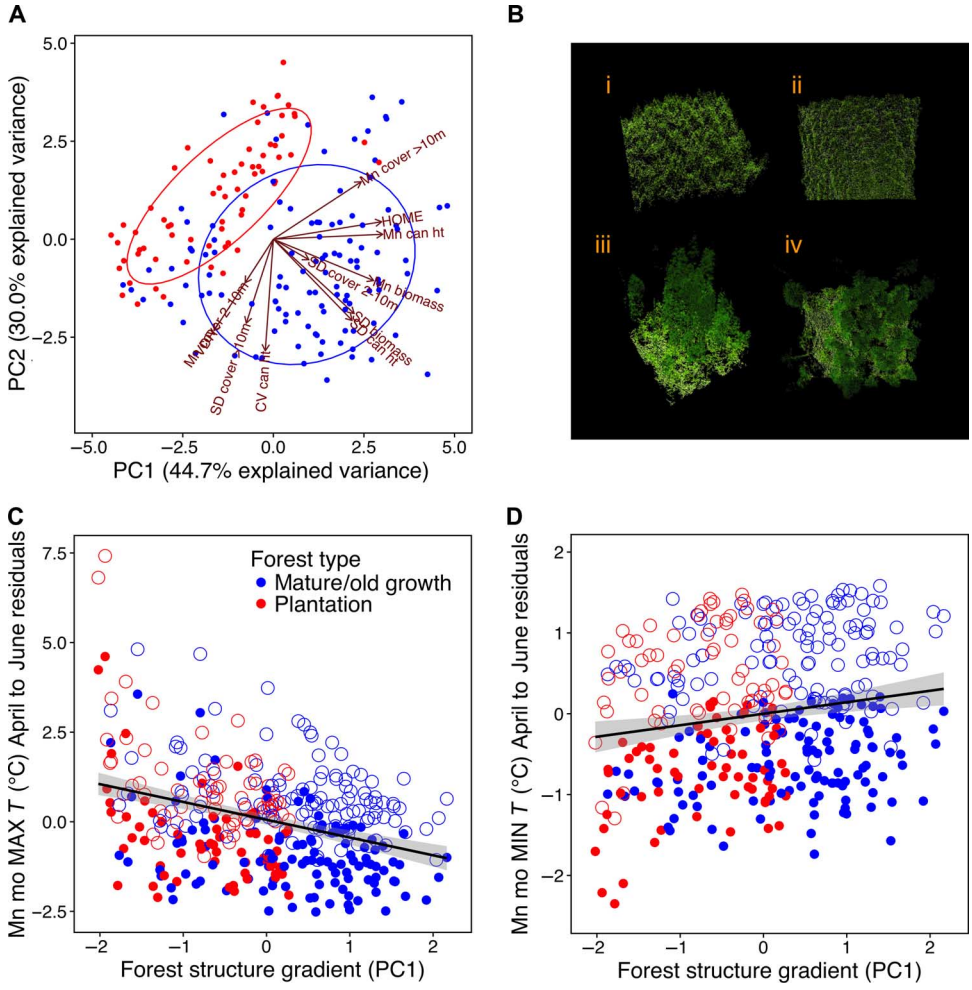

Fig. 4. Differences in microclimate conditions across a gradient in forest structure. (**A**) Principal components analysis (PCA) showing how vegetation structure metrics differ between mature/old-growth forest sites and plantations. The ellipses represent 68% of the data assuming a normal distribution in each category (plantation and mature/old growth). (**B**) Three-dimensional LiDAR-generated images of plantation forests [(i) side view; (ii) overhead view] and old-growth forests [(iii) side view; (iv) overhead view] at the Andrews Forest. (C and D) Results from generalized linear mixed models show the modeled relationship between forest structure [PC1, the first component of a PCA on forest structure variables (A)] and the residuals from an elevation-only model of mean monthly maximum during April to June (**C**) and mean monthly minimum during April to June (**D**) after accounting for the effects of elevation. Closed circles represent 2012 and open circles represent 2013. Maximum monthly temperatures (C) decreased by 2.5°C (95% confidence interval, 1.7° to 3.2°C) and observed minimum temperatures (D) increased by 0.7°C (0.3° to 1.1°C) across the observed structure gradient from plantation to old-growth forest.

Table 1. Generalized linear mixed model results for the relationship between temperature metrics and the first component of a PCA (PC1) representing a gradient in vegetation structure. Data from 2012 and 2013 were combined and "site" was included as a random effect in all models. Lower PC1 values indicate forest plantations and higher values indicate old-growth forests. "Change in temperature metrics" reports the average difference in temperature (°C) or degree days (dd) across the range of PC1 values. The effect of old-growth structure (PC1) on microclimate was consistent between years for most variables ("No year effects"). Effects of old-growth forests were stronger in 2012, and the direction of old-growth effects remained consistent for all but SD in weekly temperature. We included elevation (ELV) in all models to statistically account for elevation differences. Elevation had a significant effect on all models ($P < 0.0001$), except for SD in weekly temperature from January to March ($P = 0.062$). Coefficients from the interaction models include the 2012 intercept ($\hat{\beta}_0$ 2012), the slope of the 2012 PC1 effect ($\hat{\beta}_1$ PC1 2012), the 2013 intercept presented as the difference from the 2012 intercept ($\Delta\hat{\beta}_0$ 2013), and the 2013 PC1 effect presented as the difference from the 2012 PC1 effect (PC1 $\Delta\hat{\beta}_1$ 2013). *P* values in boldface indicate a statistically significant effect of PC1 on temperature metrics at $P < 0.05$. LCL, lower 95% confidence limit; UCL, upper 95% confidence limit.

Variable	Intercept		PC1			Change in temperature metrics ~ PC1			
	$\hat{\beta}_0$	SE	$\hat{\beta}_1$	SE	*P*	Units	Change	LCL	UCL
No year effects									
CDD > 0°C January to March	178.66	3.66	−0.47	3.92	0.9051	dd	−1.96	−37.01	14.25
CDD > 0°C April to June	820.27	4.17	−10.25	4.47	**0.0229**	dd	−42.89	−82.83	−2.95
Mn mo MEAN *T* April to June	8.98	0.05	−0.11	0.05	**0.0235**	°C	−0.47	−0.92	−0.03
Mn mo MAX *T* April to June	13.68	0.08	−0.59	0.09	**<0.0001**	°C	−2.47	−3.24	−1.70
Mn mo MIN *T* April to June	5.29	0.04	0.16	0.05	**0.0006**	°C	0.68	0.26	1.10
Significant year effects									
	Intercept 2012		PC1 2012			2012 Change in temperature metrics ~ PC1			
	$\hat{\beta}_0$	SE	$\hat{\beta}_1$	SE	*P*	Units	Change	LCL	UCL
CDD > 10°C April to June	115.06	1.73	−7.84	1.85	**<0.0001**	dd	−32.82	−49.36	−16.28
SD wkly *T* January to March	1.62	0.03	−0.07	0.03	**0.0341**	°C	−0.27	−0.55	0.00
SD wkly *T* April to June	3.78	0.01	0.01	0.01	0.4512	°C	0.03	−0.04	0.13
MAX *T* warmest mo	25.22	0.14	−0.68	0.15	**<0.0001**	°C	−2.82	−4.15	−1.49
MIN *T* coldest mo	−1.14	0.06	0.33	0.06	**<0.0001**	°C	1.39	0.88	1.91
	Intercept 2013		PC1 2013			2013 Change in temperature metrics ~ PC1			
	$\Delta\hat{\beta}_0$	SE	$\Delta\hat{\beta}_1$	SE	*P*	Units	Change	LCL	UCL
CDD > 10°C April to June	73.36	0.71	2.72	0.71	**0.0002**	dd	−21.43	−37.97	−4.90
SD wkly *T* January to March	0.98	0.04	0.13	0.04	**0.0014**	°C	0.26	0.02	−0.53
SD wkly *T* April to June	1.08	0.01	−0.04	0.01	**0.0071**	°C	−0.11	−0.21	−0.02
MAX *T* warmest mo	1.17	0.06	0.19	0.06	**0.0047**	°C	−2.05	−3.38	−0.72
MIN *T* coldest mo	−0.61	0.08	−0.26	0.08	**0.0013**	°C	0.32	0.16	0.84

reported structural differences between old-growth forests and secondary Douglas-fir (*Pseudotsuga menzisii*) forests in the Pacific Northwest (*28*).

After we statistically controlled for the effects of elevation, PC1 was associated with most temperature variables (8 of 10 variables; Table 1). Effects were largest for maximum and minimum temperatures, as well as for CDDs in the spring and summer months. Temperature differences were substantial across the gradient in forest structure; for instance, in 2012, maximum spring monthly temperatures decreased by 2.5°C (95% confidence interval, 1.7° to 3.2°C; Fig. 4C) across the observed gradient in forest structure (from structurally simple plantations to complex old-growth forests). Minimum temperatures during this same period were 0.7°C (95% confidence interval, 0.3° to 1.1°C; Fig. 4D) warmer across the same gradient. Overall, these influences of old-growth forests on thermal conditions were consistent between years (although we found statistical evidence for year × PC1 interactions, parameter estimates of the interactions tended to be small and only resulted in a sign change for variability in temperature from January to March; Table 1).

DISCUSSION

Elevation was a powerful predictor for air temperatures across years, variables, and scales, confirming the importance of macrotopography

in temperature patterns (*7*, *20*). However, although elevation predicted most temperature metrics well, it was less effective in predicting temperature variability and degree-day accumulation from January to March—both of which are microclimatic factors that are likely to influence species behavior and demography (*29*). Microtopographic variables, including slope, aspect, and relative topographic position, also influenced temperature patterns, but this effect varied markedly by time of year. Depressions and other topographically sheltered areas are thought to contribute to the decoupling of surface temperatures from regional patterns, thereby potentially generating microrefugia in complex terrain (*7*). These topographic features exerted a large influence on understory microclimate during winter, when persistent cold air pools form in depressions and valleys.

Vegetation characteristics associated with older forest stands appeared to confer a strong, thermally insulating effect. Older forests with tall canopies, high biomass, and vertical complexity (Fig. 1A) provided cooler microclimates compared with simplified stands (Fig. 1B). This resulted in differences as large as 2.5°C between plantation sites and old-growth sites, a temperature range equivalent to predicted global temperature increases over the next 50 years (*30*). This effect was potentially attributable to large differences in biomass between forest types (*16*), rather than canopy cover, as we observed less variation in canopy cover between old-growth sites and plantation sites (table S5). Although previous studies have shown strong influences of vegetation on microclimate, most of these demonstrated differences between significantly different vegetation types or stages, such as mature forests versus grasslands (*18*, *31*) or clearcuts (*19*, *32*). At the global scale, forests have been shown to have a broad-scale cooling effect (*33*); however, to our knowledge, this is the first evidence that subtler structural differences within mature forest types (that is, mature plantations versus old-growth forests) mediate under-canopy temperature regimes.

Our findings indicate that management practices that result in single-species, even-aged plantations are likely to reduce the thermal buffering capacity of forest sites, potentially limiting the availability of favorable microclimates for some species. Unlike most predictors, which were primarily useful when summarized at fine spatial scales (25-m radius), vegetation at broader scales exerted the strongest influences on temperature. This is consistent with results from studies that examine the thermal edge effects of high-contrast cover types (*34*); smaller forest patches tend to be more susceptible to changes in temperature (*20*), and such edge effects also limit microclimatic buffering of tropical forests (*22*). In jurisdictions where biodiversity maintenance is the goal, conservation and restoration of structures associated with old-growth forests are more likely to sustain favorable microclimates (*35*) and to reduce climate change impacts on temperature-sensitive species. Recent work shows that the understory microclimate differences documented here could be highly relevant to biodiversity conservation in temperate forests; cooler forest types have attenuated the widespread loss of cool-adapted understory plant species (*13*) and have promoted tree recruitment (*36*). Amphibians, lizards, insects, and even large mammals are shown to take advantage of microclimate conditions when regional climate moves beyond the range of thermal preferences (*5*, *37*, *38*). However, our findings apply to species inhabiting forest understory. Although a high proportion of forest biodiversity is found in this stratum (*39*–*41*), species associated with upper canopies may not benefit from the microclimate buffering capacity of old-growth forests. Furthermore, because older seral stages provide the highest levels of buffering, management options may be limited for species inhabiting early successional forests (*42*), unless they are able to take advantage of the microclimatic buffering of older forests or cooler microclimates that are near old-forest edges (*34*). Currently, early seral species are of high conservation concern in the Pacific Northwest, largely as a result of habitat loss (*42*); given that early seral forests may not have equivalent thermal refuges, we predict synergistic negative effects on these species when combined with climate.

We conclude that the substantial influence of vegetation structure on microclimate presents the opportunity to manage for conditions that favor the persistence of biodiversity (*43*). By conserving or creating forest conditions that buffer organisms from the impacts of regional warming and/or slow the rate at which organisms must adapt to a changing climate, it may be possible to ameliorate some of the severe negative effects of regional warming. Given the time frame for forests to acquire old-growth structural conditions, understanding thresholds in forest structure where important ecosystem services are lost is of pressing concern (*44*). With ~3.5 million ha of old-growth forests remaining in the coastal region of the Pacific Northwest (much of which is now protected under the federal Northwest Forest Plan) (*45*), there is substantial potential—in this region at least—to reduce the effects of warming on native populations of forest species.

Understanding the fine-resolution effects of vegetation structure on mediating microclimate could also improve predictions about biodiversity responses to climate change. Without considering the detailed information on forest structural conditions reported in this paper, published model estimates of changes in species' climatic niches (and extinction risk) (*46*, *47*) could be substantially underestimated or overestimated, depending on the amount of old forests in a landscape. We demonstrate how combining new remote sensing technologies (*48*) with machine-learning techniques provides an effective option to develop high-resolution, spatially explicit models of under-canopy temperature characteristics. As under-canopy temperature data become more readily available, microclimate variability can thus be mapped across broad spatial scales. Under-canopy temperature modeling, coupled with models predicting future vegetation dynamics (*49*), offers the potential to enhance our understanding of microclimate and species persistence in the face of climate change.

MATERIALS AND METHODS

Experimental design

We collected fine-scale temperature data using calibrated HOBO pendant data loggers (Supplementary Materials) at 183 locations across the 6400-ha HJA in the Cascade Mountains of central Oregon, USA (44°12′N, 122°15′W). Data loggers were placed 1.5 m above the forest floor; this ground- and shrub-level forest stratum is characterized by particularly high biodiversity in Douglas-fir forests of the Pacific Northwest (*39*–*41*). The HJA spans an elevational gradient from 410 to 1630 m above sea level. It is a conifer forest mosaic that is largely composed of a mix of old-growth forests, mature forests, and 40- to 60-year-old Douglas-fir plantations. Sampling locations were stratified across elevation, forest type, and distance to roads, ensuring that the full environmental gradient was sampled (Fig. 3) with a minimum distance between sampling points of 300 m (Supplementary Materials). We collected air temperature data at the 183 sample locations from January 2012 to July 2013. In total, we used 7,417,320 temperature loggings to calculate summary metrics (table S6).

Environmental predictor variables

To model temperature metrics, we selected 19 predictor variables (table S7) that we hypothesized to be important for influencing air temperatures in forested mountain landscapes and categorized these into three main groups: (i) elevation (ELV), (ii) microtopography (TOPO), and (iii) vegetation structure (VEG). We derived all vegetation variables from LiDAR data collected at the HJA in August 2008 during the leaf-on period (*50*). LiDAR is a relatively new technology that allows for fine-scale mapping of forest structure across broad spatial extents (*51*, *52*). The VEG category variables described vegetation structure using metrics relating to (i) canopy height, (ii) cover at multiple strata, and (iii) vertical distribution of canopy elements.

Spatial scales

We assessed the importance of our predictor variables at two spatial extents around each sample point because the scale at which drivers of microclimate act is largely unknown (*29*): (i) at a radius of 25 m, which represents local-scale predictors, and (ii) at a radius of 250 m, which represents stand-scale conditions. The relative roles of the biotic and abiotic aspects of the environment could influence microclimate differently at these two spatial scales (*3*).

Response variables

Our 10 response variables included CDDs, mean monthly minimum and maximum temperatures, and variability in temperature (table S6). CDDs are linked closely to timing of spring plant bud burst, leaf out, and flowering, as well as insect emergence, and therefore have the potential to influence higher trophic levels (*53*). Variability in weekly temperature in both time periods (as measured by SD) may also determine the quality of sites (*54*). We chose the two time periods of January to March (winter-spring transition) and April to June (spring-summer transition) because they are relevant to the phenology of many organisms on our landscape. In temperate regions, phenological events during spring also have direct implications for reproduction and growth in both plants and animals (*55*). We also included the minimum and maximum temperatures of the coldest and warmest months, respectively, as they represent extremes at the annual time scale.

Statistical analysis: BRTs

We used a machine-learning approach (BRTs) to explore the relationship between our suite of predictor variables (19 × 2 spatial scales = 38 total predictor variables; table S7) and air temperature at our 183 sample locations. BRTs have recently been used extensively in species distribution modeling because of their capacity for uncovering nonlinear relationships between predictors and response variables, as well as their flexibility in testing interactions among predictors (*25*). BRTs can also handle large numbers of predictor variables and the colinearity between them (*25*), which is advantageous in studies such as ours, where there are many categorized predictor variables (table S7) but little prior information about which are most important or at which spatial scales. This modeling method afforded the flexibility to explore multiple potential correlates of microclimate without arbitrarily restricting our predictor set. We used the R program version 3.0.1 (*56*) in combination with the "dismo" package version 0.8-17 (*57*) for all analyses (Supplementary Materials). We used predictive deviance, measured as the mean deviance from the held-out data in all folds, as our primary measure of model performance. We also tested the correlation between predicted and observed temperature metrics via a built-in 10-fold cross-validation that uses 10% independent "test" data. These tests thus represent an entirely independent test of model performance. If overfitting occurred, these tests should show low correlations between predicted and observed values. We also tested for spatial autocorrelation in our temperature data set (Supplementary Materials).

We assessed the contribution of each group of predictor variables (ELV, TOPO, and VEG) to the explained variance in temperature metrics by summing the RI values of the variables in each category (Supplementary Materials). To determine the direction and nature of the relationships between the temperature metrics and the most influential individual predictor variables (>2% RI), we examined the partial dependence plots for the visualization of the fitted functions.

Statistical analysis: PCA and generalized linear mixed models

We performed a PCA on all of our LiDAR-derived vegetation variables at the 25-m scale (13 variables) to test whether we could reliably differentiate between plantations and older forests (table S3). This also aided in determining whether our vegetation structure variables captured the gradient in forest structure present across the landscape. A weakness of BRTs is that they do not produce effect sizes (that is, regression slopes) that can be easily related to differences in response variables (degrees Celsius or degree days). Therefore, we used generalized linear mixed models [R package "nlme" (*58*)] to examine the relationship between values of principal components (reflecting a gradient in forest structure) and temperature metrics. We combined data from both years and included "site" as a random effect to account for a lack of independence within location between years. Elevation was included as a covariate in all models. We tested for a year effect on the influence of PC1 on microclimate via an interaction model. In this fashion, we were able to quantify differences in temperature across the old-growth forest structure gradient and to test for consistency between years.

SUPPLEMENTARY MATERIALS

Supplementary material for this article is available at http://advances.sciencemag.org/cgi/content/full/2/4/e1501392/DC1

Supplementary Materials and Methods

fig. S1. Fine-resolution (5 m) spatial predictions of temperature metrics at the HJA based on BRT models.

fig. S2. Partial dependence plots showing the relationship between selected microtopographic variables and microclimate.

fig. S3. Partial dependence plots showing the relationship between selected vegetation structure variables and microclimate.

fig. S4. Key interactions identified from BRT models testing the effects of elevation, microtopography, and vegetation structure on microclimate.

fig. S5. RI of variables measured at 25- and 250-m scales for each temperature metric in both years.

fig. S6. Comparison of observed microclimate data by year.

fig. S7. Comparison of predicted microclimate metrics by year.

fig. S8. Photo of the HOBO temperature sensor in the field.

table S1. BRT model settings (learning rate, number of trees), performance diagnostics (deviance, deviance SE, CV corr, CV SE), and tests for spatial autocorrelation in the BRT model residuals (Moran's *I* and *P*).

table S2. Pearson's correlation coefficients (*r*) and associated *P* values for both observed and predicted values between years.

table S3. Results from a PCA of all vegetation structure predictor variables.

table S4. Summary statistics and *t* tests showing differences in LiDAR metrics between mature plantations and mature/old-growth forests.

table S5. Results from Welch two-sample *t* tests comparing measures of biomass and canopy cover for plantation sites and mature/old-growth forest sites.
table S6. Temperature metrics used in our study and associated summary statistics.
table S7. Predictor variables used to predict patterns in microclimate metrics.
References (*59*–*65*)

REFERENCES AND NOTES

1. K. A. Potter, H. A. Woods, S. Pincebourde, Microclimatic challenges in global change biology. *Glob. Chang. Biol.* **19**, 2932–2939 (2013).
2. J. A. Wiens, D. Bachelet, Matching the multiple scales of conservation with the multiple scales of climate change. *Conserv. Biol.* **24**, 51–62 (2010).
3. C. Storlie, A. Merino-Viteri, B. Phillips, J. VanDerWal, J. Welbergen, S. Williams, Stepping inside the niche: Microclimate data are critical for accurate assessment of species' vulnerability to climate change. *Biol. Lett.* **10**, 20140576 (2014).
4. K. R. Ford, A. K. Ettinger, J. D. Lundquist, M. S. Raleigh, J. Hille Ris Lambers, Spatial heterogeneity in ecologically important climate variables at coarse and fine scales in a high-snow mountain landscape. *PLOS One* **8**, e65008 (2013).
5. J. M. Sunday, A. E. Bates, M. R. Kearney, R. K. Colwell, N. K. Dulvy, J. T. Longino, R. B. Huey, Thermal-safety margins and the necessity of thermoregulatory behavior across latitude and elevation. *Proc. Natl. Acad. Sci. U.S.A.* **111**, 5610–5615 (2014).
6. J. W. Oyler, S. Z. Dobrowski, A. P. Ballantyne, A. E. Klene, S. W. Running, Artificial amplification of warming trends across the mountains of the western United States. *Geophys. Res. Lett.* **42**, 153–161 (2015).
7. S. Z. Dobrowski, A climatic basis for microrefugia: The influence of terrain on climate. *Glob. Chang. Biol.* **17**, 1022–1035 (2011).
8. Mountain Research Initiative EDW Working Group, Elevation-dependent warming in mountain regions of the world. *Nat. Clim. Change* **5**, 424–430 (2015).
9. I.-C. Chen, J. K. Hill, R. Ohlemüller, D. B. Roy, C. D. Thomas, Rapid range shifts of species associated with high levels of climate warming. *Science* **333**, 1024–1026 (2011).
10. N. J. Rosenberg, *Microclimate: The Biological Environment* (Wiley-Interscience Publication, John Wiley & Sons, New York, 1974).
11. R. Geiger, *The Climate Near the Ground* (Harvard Univ. Press, Cambridge, MA, 1965).
12. P. R. Elsen, M. W. Tingley, Global mountain topography and the fate of montane species under climate change. *Nat. Clim. Change* **5**, 772–776 (2015).
13. P. De Frenne, F. Rodríguez-Sánchez, D. A. Coomes, L. Baeten, G. Verstraeten, M. Vellend, M. Bernhardt-Römermann, C. D. Brown, J. Brunet, J. Cornelis, G. M. Decocq, H. Dierschke, O. Eriksson, F. S. Gilliam, R. Hédl, T. Heinken, M. Hermy, P. Hommel, M. A. Jenkins, D. L. Kelly, K. J. Kirby, F. J. G. Mitchell, T. Naaf, M. Newman, G. Peterken, P. Petřík, J. Schultz, G. Sonnier, H. Van Calster, D. M. Waller, G.-R. Walther, P. S. White, K. D. Woods, M. Wulf, B. J. Graae, K. Verheyen, Microclimate moderates plant responses to macroclimate warming. *Proc. Natl. Acad. Sci. U.S.A.* **110**, 18561–18565 (2013).
14. M. C. Hansen, P. V. Potapov, R. Moore, M. Hancher, S. A. Turubanova, A. Tyukavina, D. Thau, S. V. Stehman, S. J. Goetz, T. R. Loveland, A. Kommareddy, A. Egorov, L. Chini, C. O. Justice, J. R. G. Townshend, High-resolution global maps of 21st-century forest cover change. *Science* **342**, 850–853 (2013).
15. R. L. Chazdon, Beyond deforestation: Restoring forests and ecosystem services on degraded lands. *Science* **320**, 1458–1460 (2008).
16. B. E. Potter, J. C. Zasada, Biomass, thermal inertia, and radiative freeze occurrence in leafless forests. *Can. J. For. Res.* **29**, 213–221 (1999).
17. T. R. Oke, J. M. Crowther, K. G. McNaughton, J. L. Monteith, B. Gardiner, The micrometeorology of the urban forest. *Philos. Trans. R. Soc. London Ser. B* **324**, 335–349 (1989).
18. A. J. Suggitt, P. K. Gillingham, J. K. Hill, B. Huntley, W. E. Kunin, D. B. Roy, C. D. Thomas, Habitat microclimates drive fine-scale variation in extreme temperatures. *Oikos* **120**, 1–8 (2011).
19. J. Chen, J. F. Franklin, T. A. Spies, Contrasting microclimates among clearcut, edge, and interior of old-growth Douglas-fir forest. *Agr. For. Meteorol.* **63**, 219–237 (1993).
20. T. Vanwalleghem, R. K. Meentemeyer, Predicting forest microclimate in heterogeneous landscapes. *Ecosystems* **12**, 1158–1172 (2009).
21. D. Lawrence, K. Vandecar, Effects of tropical deforestation on climate and agriculture. *Nat. Clim. Change* **5**, 27–36 (2015).
22. R. M. Ewers, C. Banks-Leite, Fragmentation impairs the microclimate buffering effect of tropical forests. *PLOS One* **8**, e58093 (2013).
23. D. B. Lindenmayer, W. F. Laurance, J. F. Franklin, Global decline in large old trees. *Science* **338**, 1305–1306 (2012).
24. R. Tropek, O. Sedláček, J. Beck, P. Keil, Z. Musilová, I. Šímová, D. Storch, Comment on "High-resolution global maps of 21st-century forest cover change". *Science* **344**, 981 (2014).
25. J. Elith, J. R. Leathwick, T. Hastie, A working guide to boosted regression trees. *J. Anim. Ecol.* **77**, 802–813 (2008).
26. T. A. Spies, K. N. Johnson, K. M. Burnett, J. L. Ohmann, B. C. McComb, G. H. Reeves, P. Bettinger, J. D. Kline, B. Garber-Yonts, Cumulative ecological and socioeconomic effects of forest policies in Coastal Oregon. *Ecol. Appl.* **17**, 5–17 (2007).
27. R. A. Fisher, The use of multiple measurements in taxonomic problems. *Ann. Eugen.* **7**, 179–188 (1936).
28. J. F. Franklin, T. A. Spies, R. V. Pelt, A. B. Carey, D. A. Thornburgh, D. R. Berg, D. B. Lindenmayer, M. E. Harmon, W. S. Keeton, D. C. Shaw, K. Bible, J. Chen, Disturbances and structural development of natural forest ecosystems with silvicultural implications, using Douglas-fir forests as an example. *For. Ecol. Manage.* **155**, 399–423 (2002).
29. J. Bernardo, Biologically grounded predictions of species resistance and resilience to climate change. *Proc. Natl. Acad. Sci. U.S.A.* **111**, 5450–5451 (2014).
30. Intergovernmental Panel on Climate Change, *Climate Change 2014: Impacts, Adaptation, and Vulnerability. Part A: Global and Sectoral Aspects. Contribution of Working Group II to the Fifth Assessment Report of the Intergovernmental Panel on Climate Change* (Cambridge Univ. Press, Cambridge, 2014).
31. P. D'Odorico, Y. He, S. Collins, S. F. J. De Wekker, V. Engel, J. D. Fuentes, Vegetation–microclimate feedbacks in woodland–grassland ecotones. *Glob. Ecol. Biogeogr.* **22**, 364–379 (2013).
32. T. D. Heithecker, C. B. Halpern, Edge-related gradients in microclimate in forest aggregates following structural retention harvests in western Washington. *For. Ecol. Manage.* **248**, 163–173 (2007).
33. Y. Li, M. Zhao, S. Motesharrei, Q. Mu, E. Kalnay, S. Li, Local cooling and warming effects of forests based on satellite observations. *Nat. Commun.* **6**, 6603 (2015).
34. T. P. Baker, G. J. Jordan, E. A. Steel, N. M. Fountain-Jones, T. J. Wardlaw, S. C. Baker, Microclimate through space and time: Microclimatic variation at the edge of regeneration forests over daily, yearly and decadal time scales. *For. Ecol. Manage.* **334**, 174–184 (2014).
35. R. Julliard, F. Jiguet, D. Couvet, Common birds facing global changes: What makes a species at risk? *Glob. Chang. Biol.* **10**, 148–154 (2004).
36. S. Z. Dobrowski, A. K. Swanson, J. T. Abatzoglou, Z. A. Holden, H. D. Safford, M. K. Schwartz, D. G. Gavin, Forest structure and species traits mediate projected recruitment declines in western US tree species. *Glob. Ecol. Biogeogr.* **24**, 917–927 (2015).
37. R. A. Long, R. T. Bowyer, W. P. Porter, P. Mathewson, K. L. Monteith, J. G. Kie, Behavior and nutritional condition buffer a large-bodied endotherm against direct and indirect effects of climate. *Ecol. Monogr.* **84**, 513–532 (2014).
38. B. R. Scheffers, R. M. Brunner, S. D. Ramirez, L. P. Shoo, A. Diesmos, S. E. Williams, Thermal buffering of microhabitats is a critical factor mediating warming vulnerability of frogs in the Philippine biodiversity hotspot. *Biotropica* **45**, 628–635 (2013).
39. J. C. Hagar, Wildlife species associated with non-coniferous vegetation in Pacific Northwest conifer forests: A review. *For. Ecol. Manage.* **246**, 108–122 (2007).
40. H. T. Root, M. G. Betts, Managing moist temperate forests for bioenergy and biodiversity. *J. For.* **114**, 66–74 (2016).
41. F. S. Gilliam, The ecological significance of the herbaceous layer in temperate forest ecosystems. *BioScience* **57**, 845–858 (2007).
42. M. G. Betts, G. J. Forbes, A. W. Diamond, Thresholds in songbird occurrence in relation to landscape structure. *Conserv. Biol.* **21**, 1046–1058 (2007).
43. T. Oliver, D. B. Roy, J. K. Hill, T. Brereton, C. D. Thomas, Heterogeneous landscapes promote population stability. *Ecol. Lett.* **13**, 473–484 (2010).
44. S. Trumbore, P. Brando, H. Hartmann, Forest health and global change. *Science* **349**, 814–818 (2015).
45. J. R. Stritthol, D. A. Dellasala, H. Jiang, Status of mature and old-growth forests in the Pacific Northwest. *Conserv. Biol.* **20**, 363–374 (2006).
46. C. D. Thomas, A. Cameron, R. E. Green, M. Bakkenes, L. J. Beaumont, Y. C. Collingham, B. F. N. Erasmus, M. F. de Siqueira, A. Grainger, L. Hannah, L. Hughes, B. Huntley, A. S. van Jaarsveld, G. F. Midgley, L. Miles, M. A. Ortega-Huerta, A. Townsend Peterson, O. L. Phillips, S. E. Williams, Extinction risk from climate change. *Nature* **427**, 145–148 (2004).
47. A. T. Peterson, M. A. Ortega-Huerta, J. Bartley, V. Sánchez-Cordero, J. Soberón, R. H. Buddemeier, D. R. B. Stockwell, Future projections for Mexican faunas under global climate change scenarios. *Nature* **416**, 626–629 (2002).
48. R. A. Rose, D. Byler, J. R. Eastman, E. Fleishman, G. Geller, S. Goetz, L. Guild, H. Hamilton, M. Hansen, R. Headley, J. Hewson, N. Horning, B. A. Kaplin, N. Laporte, A. Leidner, P. Leimgruber, J. Morisette, J. Musinsky, L. Pintea, A. Prados, V. C. Radeloff, M. Rowen, S. Saatchi, S. Schill, K. Tabor, W. Turner, A. Vodacek, J. Vogelmann, M. Wegmann, D. Wilkie, C. Wilson, Ten ways remote sensing can contribute to conservation. *Conserv. Biol.* **29**, 350–359 (2015).
49. D. Purves, S. Pacala, Predictive models of forest dynamics. *Science* **320**, 1452–1453 (2008).
50. Watershed Sciences, T. Spies, *LiDAR Data (August 2008) for the HJ Andrews Experimental Forest and Willamette National Forest study areas. Long-term Ecological Research, Forest Science Data Bank* (Corvallis, OR, 2013); http://andrewsforest.oregonstate.edu/data/abstract.cfm?dbcode=GI010 [accessed 1 October 2013].
51. J. E. Means, S. A. Acker, B. J. Fitt, M. Renslow, L. Emerson, C. J. Hendrix, Predicting forest stand characteristics with airborne scanning lidar. *Photogramm. Eng. Remote Sens.* **66**, 1367–1371 (2000).

52. S. Goetz, D. Steinberg, R. Dubayah, B. Blair, Laser remote sensing of canopy habitat heterogeneity as a predictor of bird species richness in an eastern temperate forest, USA. *Remote Sens. Environ.* **108**, 254–263 (2007).
53. C. Both, M. van Asch, R. G. Bijlsma, A. B. van den Burg, M. E. Visser, Climate change and unequal phenological changes across four trophic levels: Constraints or adaptations? *J. Anim. Ecol.* **78**, 73–83 (2009).
54. D. Stralberg, D. Jongsomjit, C. A. Howell, M. A. Snyder, J. D. Alexander, J. A. Wiens, T. L. Root, Re-shuffling of species with climate disruption: A no-analog future for California birds? *PLOS One* **4**, e6825 (2009).
55. C. Both, R. G. Bijlsma, M. E. Visser, Climatic effects on timing of spring migration and breeding in a long-distance migrant, the pied flycatcher *Ficedula hypoleuca*. *J. Avian Biol.* **36**, 368–373 (2005).
56. R Development Core Team, *R: A Language and Environment for Statistical Computing* (R Foundation for Statistical Computing, Vienna, Austria, 2011).
57. R. J. Hijmans, S. Phillips, J. Leathwick, J. Elith, "dismo: Species distribution modeling. R package version 0.8-17"; http://CRAN.R-project.org/package=dismo [accessed 12 September 2013].
58. J. Pinheiro, D. Bates, S. DebRoy, D. Sarkar, R Core Team, "nlme: Linear and Nonlinear Mixed Effects Models. R package version 3.1-125"; https://cran.r-project.org/web/packages/nlme [accessed 1 March 2016].
59. H. L. Beyer, "Hawth's Analysis Tools for ArcGIS"; www.spatialecology.com/htools [accessed 1 March 2009].
60. ESRI, *ArcGIS Desktop: Release 10* (Environmental Systems Research Institute, Redlands, CA, 2011).
61. J. Elith, J. R. Leathwick, *Boosted Regression Trees for Ecological Modeling. R Vignette for Package 'Dismo'* (2014); https://cran.r-project.org/web/packages/dismo/vignettes/brt.pdf [accessed 1 November 2014].
62. P. Legendre, Spatial autocorrelation: Trouble or new paradigm. *Ecology* **74**, 1659–1673 (1993).
63. O. N. Bjornstad, "ncf: Spatial nonparametric covariance functions. R package version 1.1-5"; http://CRAN.R-project.org/package=ncf [accessed 1 October 2014].
64. C. Daly, D. R. Conklin, M. H. Unsworth, Local atmospheric decoupling in complex topography alters climate change impacts. *Int. J. Climatol.* **30**, 1857–1864 (2010).
65. S. J. Goetz, D. Steinberg, M. G. Betts, R. T. Holmes, P. J. Doran, R. Dubayah, M. Hofton, Lidar remote sensing variables predict breeding habitat of a Neotropical migrant bird. *Ecology* **91**, 1569–1576 (2010).

Acknowledgments: We extend our special thanks to T. Valentine for her help with GIS (geographic information system), to C. Murphy and E. Miles for assistance with the temperature data processing, and to J. Sexton for providing logistical support for field work. We also thank C. Still, whose comments greatly improved this manuscript. This work would not have been possible without our field assistants (E. Jackson, A. Bartelt, S. Ashe, S. Yegorova, A. Mott, and K. Stanley). **Funding:** This research was made possible with support from multiple grants and awards: an NSF–Integrative Graduate Education and Research Traineeship fellowship (NSF-0333257), a Department of the Interior Northwest Climate Science Center graduate fellowship, and an Andrews Forest Long-Term Ecological Research graduate research assistantship (NSF DEB-0823380) all awarded to S.J.K.F. Research and support were provided by the HJA research program, funded by the NSF's Long-Term Ecological Research Program (NSF DEB-0823380), the U.S. Forest Service Pacific Northwest Research Station, and Oregon State University. The project described in this publication was also supported by a grant awarded to M.G.B. from the Department of the Interior through Cooperative Agreement No. G11AC20255 from the U.S. Geological Survey and an NSF grant awarded to M.G.B. and J.J. (NSF ARC-0941748). The contents of this paper are solely the responsibility of the authors and do not represent the views of the Northwest Climate Science Center, the U.S. Geological Survey, or the U.S. Forest Service. **Author contributions:** S.J.K.F. and M.G.B. conceived the study and planned the analysis. S.J.K.F. analyzed the data. S.J.K.F., M.G.B., and A.S.H. co-wrote the manuscript. S.J.K.F. and A.S.H. collected the data. All authors discussed the results and edited and commented on the manuscript. **Competing interests:** The authors declare that they have no competing interests. **Data and materials availability:** All data needed to evaluate the conclusions in the paper are present in the paper and/or the Supplementary Materials. Air temperature and LiDAR data are available online at the Andrews Forest Webpage (air temperature: http://andrewsforest.oregonstate.edu/data/abstract.cfm?dbcode=MS045; LiDAR: http://andrewsforest.oregonstate.edu/data/abstract.cfm?dbcode=GI010). Additional data related to this paper may be requested from the authors.

Submitted 6 October 2015
Accepted 25 March 2016
Published 22 April 2016
10.1126/sciadv.1501392

Citation: S. J. K. Frey, A. S. Hadley, S. L. Johnson, M. Schulze, J. A. Jones, M. G. Betts, Spatial models reveal the microclimatic buffering capacity of old-growth forests. *Sci. Adv.* **2**, e1501392 (2016).

ScienceAdvances
AAAS

Spatial models reveal the microclimatic buffering capacity of old-growth forests

Sarah J. K. Frey, Adam S. Hadley, Sherri L. Johnson, Mark Schulze, Julia A. Jones and Matthew G. Betts (April 22, 2016)

Sci Adv 2016, 2:.
doi: 10.1126/sciadv.1501392